molecular pharmaceutics

ARTICLE

pubs.acs.org/molecularpharmaceutics

Cocrystals of Quercetin with Improved Solubility and Oral Bioavailability

Adam J. Smith,[†,‡] Padmini Kavuru,[§] Lukasz Wojtas,[§] Michael J. Zaworotko,[*,§] and R. Douglas Shytle[*,†,‡]

[†]Center of Excellence for Aging and Brain Repair, Department of Neurosurgery and Brain Repair, USF Health College of Medicine, [‡]Neuroimmunology Laboratory, Silver Child Development Center, Department of Psychiatry and Neurosciences, USF Health College of Medicine, and [§]Department of Chemistry, College of Arts and Sciences, University of South Florida, Tampa, Florida

Supporting Information

ABSTRACT: Flavonoids have been studied extensively due to the observation that diets rich in these compounds are associated with lower incidences of many diseases. One of the most studied flavonoids, quercetin, is also the most abundant of these compounds in the plant kingdom. Numerous therapeutic bioactivities have been identified *in vitro*. However, its *in vivo* efficacy in pure form is limited by poor bioavailability, primarily due to its low solubility and consequent low absorption in the gut. Cocrystallization has gained attention recently as a means for improving the physicochemical characteristics of a compound. Here, we synthesized and evaluated four new cocrystals of quercetin (QUE): quercetin:caffeine (QUECAF), quercetin:caffeine:methanol (QUECAF·MeOH), quercetin:isonicotinamide (QUEINM), and quercetin:theobromine dihydrate (QUETBR·$2H_2O$). Each of these cocrystals exhibited pharmacokinetic properties that are vastly superior to those of quercetin alone. Cocrystallization was able to overcome the water insolubility of quercetin, with all four cocrystals exhibiting some degree of solubility. The QUECAF and QUECAF·MeOH cocrystals increased the solubility of QUE by 14- and 8-fold when compared to QUE dihydrate. We hypothesized that this improved solubility would translate into enhanced systemic absorption of QUE. This hypothesis was supported in our pharmacokinetic study. The cocrystals outperformed QUE dihydrate with increases in bioavailability up to nearly 10-fold.

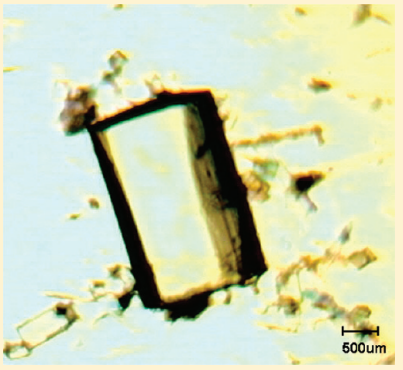

KEYWORDS: quercetin, cocrystal, bioavailability, solubility, pharmacokinetics

INTRODUCTION

Flavonoids in general are widely studied and have been found to promote healthy living in epidemiologic studies.[1,2] Quercetin, 3,3′,4′,5,7-pentahydroxyflavone (QUE), is one of the most common dietary flavonoids and is found throughout the plant kingdom (Figure 1). A typical Western diet was estimated to provide between 0 and 30 mg of QUE per day, most of which is consumed as tea, red wine, fruits and vegetables.[3] This not only supports its safety for consumption by humans (albeit at a low dose) but also provides epidemiological evidence for its beneficial effects. QUE is perhaps best known for its antioxidant activity but has numerous other biological and pharmacological effects including metal chelation, anticarcinogenic, cardioprotective, bacteriostatic, and antiviral activity.[4−9]

Even though QUE has been found to have many potential beneficial effects, its usefulness *in vivo* is questionable due to unfavorable pharmacokinetics in its pure form. The bioavailability of QUE has been studied extensively.[10−18] Unfortunately, it appears that QUE is absorbed poorly, is highly susceptible to metabolic conjugation, and exists mostly as a conjugated form in systemic circulation, resulting in low bioavailability.[10,18] Furthermore, QUE bioavailability has been evaluated in humans following a single 4 g oral dose. The investigators reported that, following oral administration, no measurable plasma or urine QUE concentrations could be detected.[19] They concluded that less than 1% of the QUE was absorbed unchanged in the gastrointestinal tract.[19] This is not surprising given that QUE has extremely low water solubility, a major factor in drug absorption. Not only is QUE absorbed poorly but also it is conjugated extensively in the liver following oral administration.[10,17,20] In dogs, more than 80% of the circulating flavonols existed as conjugated metabolites.[20] Since many of the proposed health effects of QUE were observed *in vitro* with the unconjugated aglycon, it is questionable whether the QUE metabolites will remain bioactive. Few investigators have studied the bioactivity of QUE metabolites, and those that do typically only look at one potential clinical indication for QUE. Spencer et al. studied the bioactivity of *in vivo* QUE metabolites. They found that 3′-*O*-methyl quercetin and 4′-*O*-methyl quercetin had a reduced capacity to protect fibroblasts from peroxide-induced cell damage, whereas quercetin 7-*O*-*β*-D-glucuronide was completely inactive.[6] Even though this study only investigated one activity of QUE, it is probable that the *in vivo* effectiveness of QUE will be limited by its absorption and metabolism.

Thus, novel strategies that can increase the absorption of QUE or affect its metabolism are desirable. The pharmaceutical industry typically employs several methods for correcting compounds

Received: April 25, 2011
Accepted: August 16, 2011
Revised: July 14, 2011
Published: August 16, 2011

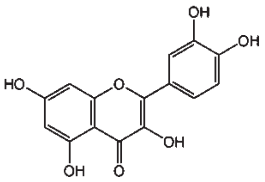

Figure 1. Structure of quercetin.

that exhibit undesirable physicochemical characteristics including screening for salts, polymorphs, and hydrates/solvates of the active pharmaceutical ingredient (API).[21] However, one long known methodology has remained relatively unexplored by many. Cocrystallization is beginning to attract the attention of the pharmaceutical industry because it can be used to both modify the physicochemical properties of a compound without affecting the intrinsic bioactivity and extend the product life of the API.[22] Cocrystals have been defined as "a multiple component crystal in which all components are solid under ambient conditions when in their pure form".[21] The API and cocrystal former(s) exist at a stoichiometric ratio and form complexes that are generally stabilized by hydrogen bonds. This technique has been used to improve the physicochemical properties of numerous different APIs.[23−31] Most notably, cocrystallization is often used to modulate the solubility of an API. Whenever solubility is a limiting factor in the bioavailability of a compound (like with QUE), modulation of solubility can produce drastic effects. Thus, we determined that QUE would be a good candidate for cocrystallization.

In this report, we evaluate the solubility and pharmacokinetic profile of four novel QUE cocrystals. Each of the cocrystals described was selected due to improved physicochemical properties that we hypothesized would lead to improved bioavailability.

EXPERIMENTAL SECTION

Reagents and Materials. Quercetin dihydrate (98% purity), isonicotinamide (INM) (99% purity), caffeine (CAF), and theobromine (TBR) (98% purity) were purchased from Sigma-Aldrich Corporation (St. Louis, MO, USA).

Synthesis of the Cocrystals. The cocrystal reaction scheme has been illustrated in Figure 2.

QUECAF·MeOH. QUE dihydrate (34.0 mg, 0.101 mmol) and CAF (19.0 mg, 0.100 mmol) were dissolved in 6 mL of methanol by heating. The resulting solution was placed in a refrigerator overnight. Golden yellow crystals of the cocrystal were harvested (melting point = 246 °C).

QUECAF. The cocrystal was prepared by desolvating QUECAF·MeOH. It was prepared by overnight slurrying of QUE dihydrate (101.46 mg, 0.300 mmol) and caffeine (58.23 mg, 0.300 mmol) in 2 mL of methanol. The solid was filtered and dried in the vacuum oven for 3 h at 150 °C, thereby affording QUECAF (melting point of dried solid = 245.95 °C).

QUEINM. QUE dihydrate (34.0 mg, 0.101 mmol) and INM (12.3 mg, 0.100 mmol) were dissolved in 6 mL of methanol by heating on a hot plate. The resulting solution was placed in a refrigerator. After 2 days, yellow plate crystals of QUEINM were obtained (melting point = 262 °C).

QUETBR·2H_2O. QUE dihydrate (33.8 mg, 0.099 mmol) and TBR (18.0 mg, 0. 099 mmol) were dissolved in 5 mL of ethanol and 10 mL of 1:1 mixture of water and ethanol respectively by heating. Resulting solutions were filtered together and placed in the refrigerator for slow evaporation. The crystals were harvested after 4 days (melting point = 293.8 °C).

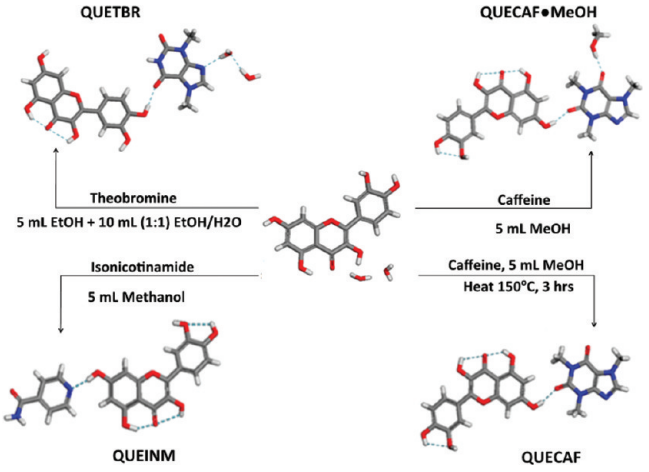

Figure 2. Cocrystal reaction scheme. Hydrogen bonds are indicated by blue, dashed lines.

Synthesis of Cocrystals in Bulk for Dissolution. The cocrystals were made in bulk for dissolution study by a slurry method. For each cocrystal stoichiometric amounts of the starting materials in 5−6 mL of methanol were combined and stirred overnight with the help of a magnetic stir bar on a stir plate, which produces the cocrystals in 100% yield. The purity of the bulk material is tested by powder X-ray diffraction (PXRD) and differential scanning calorimetry (DSC). For PXRD the pattern of the bulk material is compared to the PXRD obtained from the single crystal X-ray diffraction, and the presence of any additional peaks other than the peaks in the calculated pattern indicates starting materials or impurities. Likewise, DSC of the bulk cocrystal exhibits an endotherm for the melting point of the cocrystals and the desolvation/dehydration.

Differential Scanning Calorimetry (DSC). Thermal analysis was performed on a TA Instruments DSC 2920 differential scanning calorimeter. Aluminum pans were used for all samples, and the instrument was calibrated using an indium standard. For reference, an empty pan sealed in the same way as the sample was used. Using inert nitrogen conditions, the samples were heated in the DSC cell from 30 °C to the required temperature (melting point of the cocrystal) at a rate of 10 °C/min.

Infrared Spectroscopy (FT-IR). To characterize the cocrystals by infrared spectroscopy a Nicolet Avatar 320 FT-IR instrument was used. Sample amounts of 1−2 mg were used, and spectra were measured over the range of 4000−400 cm^{-1} and analyzed using EZ Omnic software.

Ultraviolet/Visible Spectroscopy (UV/Vis). UV/vis analysis was performed on a Perkin-Elmer Lambda 900 UV/vis/NIR spectrometer.

Powder X-ray Diffraction (PXRD). A Bruker AXS D8 powder diffractometer was used for all PXRD measurements with experimental parameters as follows: Cu Kα radiation (λ = 1.54056 Å); 40 kV and 30 mA. Scanning interval: 3−40° 2θ. Time per step: 0.5 s. The experimental PXRD patterns and calculated PXRD patterns from single crystal structures were compared to confirm the composition of bulk materials.

Single-Crystal X-ray Data Collection and Structure Determinations. Suitable crystals for X-ray crystallography were selected using an optical microscope. The X-ray diffraction data were collected on a Bruker-AXS SMART-APEXII CCD diffractometer using Cu Kα (λ = 1.54178 Å) for QUECAF·MeOH and Mo Kα radiation (λ = 0.71073 Å) for QUEINM (Table 2). Indexing was performed using APEX2[32] (difference vectors method). Data integration and reduction were performed using SaintPlus 6.01.[33] Absorption correction was performed by a multiscan method implemented in SADABS.[34] Space groups were determined using XPREP implemented in APEX2.[32] The structure was solved using SHELXS-97 (direct methods) and refined using SHELXL-97 (full-matrix least-squares on F^2) contained in APEX2[32] and WinGX v1.70.01[35−37] program packages. All non-hydrogen atoms were refined anisotropically. Hydrogen atoms were placed in geometrically calculated positions and included in the refinement process using a riding model with isotropic thermal parameters: Uiso(H) = 1.5Ueq(−CH3,−OH), Uiso(H) = 1.2Ueq(−CH). Hydrogen atoms of the NH_2 group were found on a difference Fourier map and were freely refined.

Cocrystal Solubility Evaluation. Solubility studies were performed on QUECAF·MeOH, QUECAF, QUEINM, and QUETBR·2H_2O using a 1:1 mixture of water and ethanol as QUE could not be quantified by using UV/vis/NIR spectrophotometry in water alone. However the solubility of QUE and its dihydrate in water has been reported by Srinivas et al. as 0.00215 mg/mL and 0.00263 mg/mL, respectively.[38] Each of the cocrystals was synthesized in bulk by taking stoichiometric ratios of the starting materials in methanol and slurrying them for 24 h, which produced the cocrystals in 100% yield. The slurries were dried at room temperature and were sieved to attain a particle size between 53 and 75 μm. The solubility studies were conducted by taking approximately 4 g of the cocrystal in 70 mL of 50% ethanol and were stirred with a magnetic stir bar at ca. 125 rmp for 24 h at room temperature. Aliquots were drawn from the slurry at regular time intervals (5, 10, 15, 20, 25, 30, 35, 40, 45, 50, 55, 60, 75, 90, 105, 120, 150, 180, 240, and 1440 min) and filtered using 0.45 μm nylon filters. The filtrates were immediately diluted appropriately and were analyzed to measure the concentration of QUE by using a UV/vis/NIR spectrometer at 360 nm where the interference of the cocrystal formers was not observed. The remaining solids were analyzed by PXRD and DSC. The solubility measurements were done in replicates of three.

Pharmacokinetic Screening of Quercetin Formulations in Rats. Male Sprague−Dawley rats (n = 3 per group) weighing 200−250 g were purchased from Harlan Laboratories (Indianapolis, IN). The rats were purchased precannulated by Harlan. The rounded tip catheters were surgically implanted into the jugular vein of the rats making multiple, precise blood draws painless to the animal. The rats were food (not water) deprived for 18 h prior to the start of the experiment. Vegetable oil was selected as the gavage vehicle because all crystal forms were observed to be insoluble in it. The QUE formulations were delivered *via* oral gavage at a dosage of 100 mg of quercetin/kg body weight. Blood was collected at the following time points: 0, 5, 10, 30, 60, 120, 240, and 480 min. Because heparin was kept in the catheter lines to prevent clotting, a small amount of blood was drawn and discarded before collecting each sample. Approximately 300 μL of blood was collected in EDTA tubes for each time point. The samples were kept on ice to preserve their integrity and then centrifuged at 4000 rpm for 10 min, after which the plasma was transferred to sterile centrifuge tubes. A preservative solution was added to each plasma sample at 10% (v/v) concentration to ensure the integrity of the QUE during storage.[39] This preservative was composed of 20% ascorbic acid (to prevent oxidation) and 0.1% EDTA (to scavenge any metal contaminants). The samples were stored at −80 °C until they were analyzed for QUE content.

Quantification of QUE in Rat Plasma. The plasma samples were analyzed for QUE content by the Burnham Institute for Medical Research Pharmacology Core (Orlando, FL). To accurately quantify the concentration of QUE in the plasma, a previously described method was employed using liquid chromatography with tandem mass spectrometry.[40] The standards were prepared as follows. A 2.00 mg/mL stock solution of QUE was accurately prepared in DMSO. The stock solution was protected from light using amber vials and stored at −20 °C. Standards were prepared using the appropriate blank rat plasma with the ascorbic acid and EDTA preservative. The samples were aliquotted into prelabeled 1.7 mL microcentrifuge tubes. 100 μL was used as the aliquot volume for all samples. Except for the double blanks, 400 μL of the internal standard spiking solution (Naproxen, 2.00 μg/mL in ACN) was added to all samples. Tubes were then capped, vortexed for 3 min and centrifuged for 10 min at 14,000 rpm. Approximately 300 μL was then transferred from each tube into a 96-well plate for analysis by LCMSMS. The concentration range of the standard curve was 10 μg/mL to 0.100 μg/mL of QUE. The results indicated that the standard curve performance was within acceptable range for bioanalytical method acceptance (R^2> 0.99).[41−43]

Pharmacokinetic Calculations. Mean plasma QUE concentrations and the standard error in the mean (SEM) were graphed using GraphPad PRISM software (GraphPad Software, Inc.). Pharmacokinetic parameters were determined using a commercially available computer modeling program, PK Solutions v2.0.7 (Summit Research Services, Ashland, OH). The reported pharmacokinetic parameters included C_{MAX}, T_{MAX}, area under curve (AUC), relative bioavailability (F_{REL}), absorption half-life (A $T_{1/2}$), distribution half-life (D $T_{1/2}$), and elimination half-life (E $T_{1/2}$). Relative bioavailability was determined by dividing the AUC of each QUE formulation by the control.

Statistical Analysis. A post hoc t test with Bonferroni correction was used to assess the statistical significance at each time point for the pharmacokinetic study. Each QUE cocrystal was compared to the QUE dihydrate control. The criterion for rejection of the null hypothesis was $P < 0.05$.

RESULTS

Dissolution Study of the QUE Cocrystals. QUE has very poor water solubility. In fact, when we tried to determine the water solubility of QUE dihydrate, it was below our lower limit of detection. Therefore, a 1:1 ethanol/water solvent mixture was used for the dissolution studies. The solubility of QUE dihydrate in a 1:1 ethanol/water solvent mixture is found to be 0.267 mg/mL. We found that the QUECAF and QUECAF·MeOH cocrystals exhibit the highest solubilities. The maximum solubilities exhibited by QUECAF, QUECAF·MeOH, QUEINM, and QUETBR·2H_2O cocrystals were 3.627, 2.018, 1.22, and 0.326 mg/mL respectively. From the dissolution profiles it is evident that QUECAF (desolvated form of QUECAF·MeOH) displayed the highest concentration of QUE. This cocrystal increased

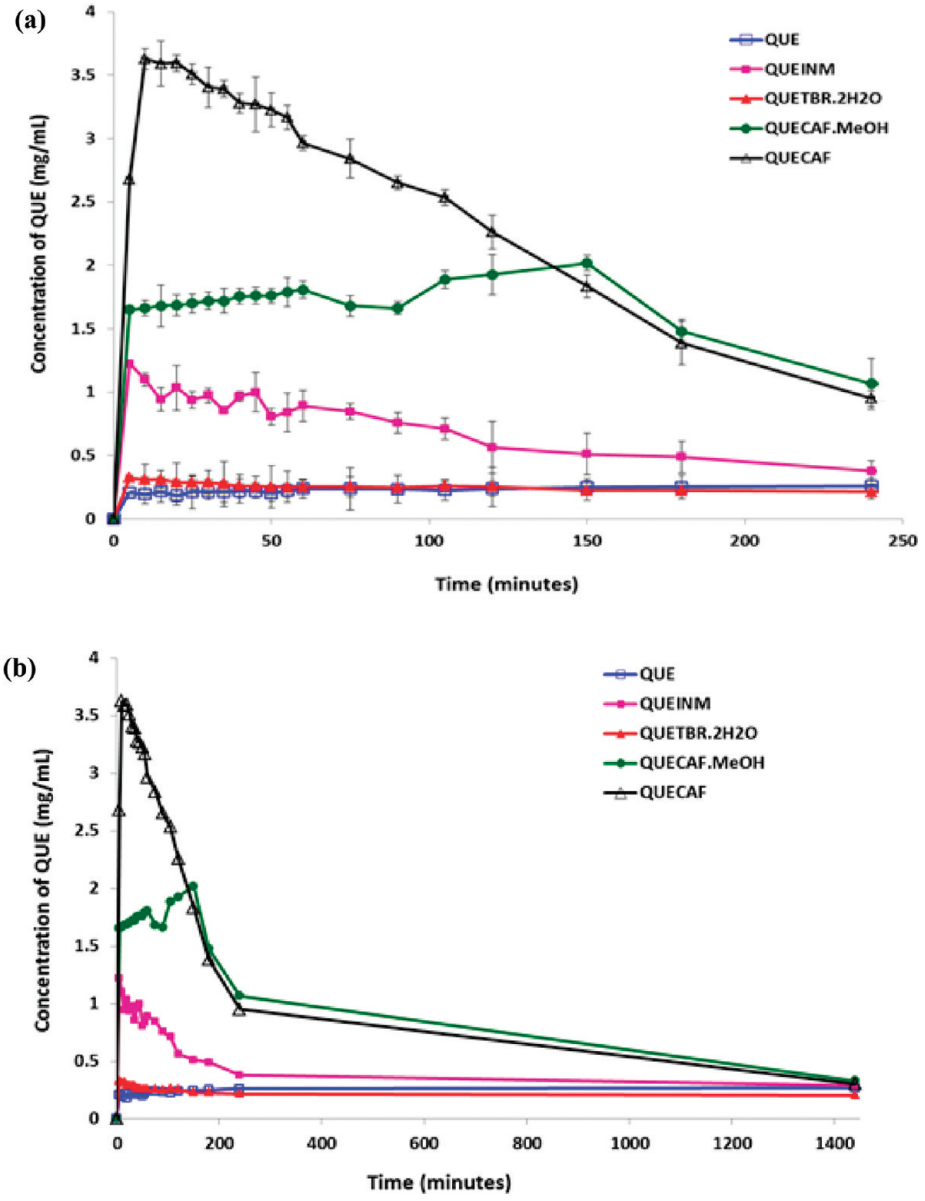

Figure 3. Dissolution profiles of QUE dihydrate and its cocrystals in 1:1 ethanol/water mixture after (a) the first 4 h and (b) 24 h.

the solubility of QUE by 14-fold, and the lowest was by QUETBR·2H_2O, which was only slightly improved over QUE alone. Figure 3a represents the dissolution profiles of QUE dihydrate and its cocrystals in the first 4 h, and Figure 3b in 24 h. The DSC and PXRD obtained from the leftover powders after 24 h dissolution reveal that QUECAF, QUECAF·MeOH, QUETBR·2H_2O and QUEINM convert back to QUE dihydrate.

Pharmacokinetics of the QUE Cocrystals . We hypothesized that the improvements in solubility would lead to improved bioavailability for the QUE cocrystals. This hypothesis was supported in our preliminary pharmacokinetic evaluation. The pharmacokinetic curves are shown in Figure 4. As expected, the QUE dihydrate was absorbed very poorly. In fact, only one of the three rats exhibited levels of QUE that were above our lower limit of quantification (0.100 μg/mL) and only at one time point, the T_{MAX}, t = 30 min. This is easily explained by the extremely poor solubility of QUE dihydrate. Because the QUE dihydrate was so poorly absorbed, we were unable to calculate half-life values for the three pharmacokinetic phases (absorption, distribution, and elimination). All four of the cocrystals exhibited favorable solubility and improved pharmacokinetic parameters. These pharmacokinetic parameters including the T_{MAX}, C_{MAX}, AUC, F_{REL}, A $T_{1/2}$, D $T_{1/2}$, and E $T_{1/2}$ can be found in Table 1. Interestingly, the QUETBR·2H_2O cocrystal was only slightly more soluble than QUE dihydrate but exhibited vastly superior pharmacokinetic properties. The QUETBR·2H_2O cocrystal had the highest F_{REL} at 9.93. This means that the AUC was nearly 10-fold higher than with QUE dihydrate. Additionally, the elimination of QUETBR·2H_2O appears to be slowed. The E $T_{1/2}$ was the highest for this cocrystal at 145 min (Table 1). All of the cocrystals reached systemic circulation more quickly than the QUE control, which is consistent with the improved solubility. Perhaps most importantly, the relative bioavailability (F_{REL}) was much higher with the cocrystals. QUEINM had the second greatest F_{REL} at 5.46, followed by the QUECAF·MeOH and

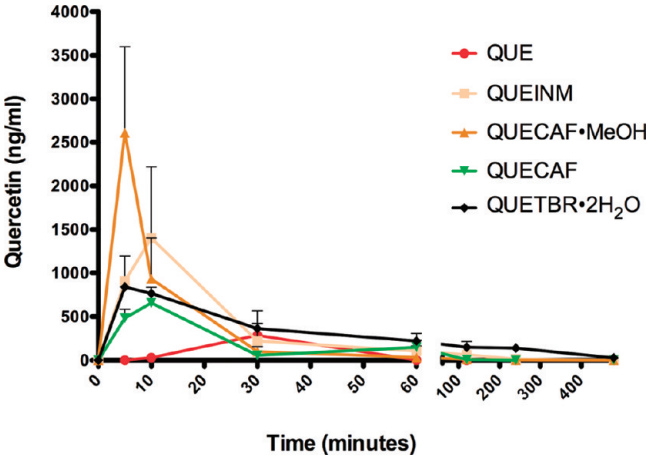

Figure 4. Pharmacokinetic profiles (mean plasma concentration + SEM versus time). There were $n = 3$ rats per group. Statistical significance was achieved for QUEINM at $t = 10$ ($p < 0.01$) and for QUECAF·MeOH at $t = 5$ ($p < 0.001$).

Table 1. Pharmacokinetic Parameters

	QUE	QUEINM	QUECAF·MeOH	QUECAF	QUETBR·2H$_2$O
T_{MAX} (min)	30	10	5	10	5
C_{MAX} (ng/mL)	285	1401	2612	656	840
AUC (ng·min/mL)	7493	40921	30084	19232	74430
F_{REL}	1	5.46	4.01	2.57	9.93
A $T_{1/2}$ (min)	n/a	3.260	2.378	2.682	1.656
D $T_{1/2}$ (min)	n/a	5.291	5.091	3.568	8.610
E $T_{1/2}$ (min)	n/a	76.934	52.447	26.381	145.309

QUECAF at 4.01 and 2.57, respectively. The E $T_{1/2}$ followed the same trend as the F_{REL}. The QUEINM exhibited an E $T_{1/2}$ of 77 min, and the QUECAF·MeOH and QUECAF cocrystals were 52 and 26 min, respectively.

Crystal Structures of the QUE Cocrystals. *QUEINM.* The 1:1 cocrystal of QUEINM contains two molecules of QUE and INM in the unit cell and crystallizes in $P\bar{1}$ space group. The catechol moiety of QUE molecules forms the O···O−H supramolecular homosynthon with hydrogen bond distance of 2.765 (3) Å (Table 3). The carbonyl and the syn-hydrogens of the amide functionality of INM molecules hydrogen bond to the catechol dimer on either side, and this results in the formation of a ring described by the R_2^2 (8) graph set[44] (N−H···O, 2.610 (3); O···O−H, 3.028 (4) Å). Thus, a four-component assembly is generated by two molecules of INM and QUE molecules which can be described by the R_4^4 (18) graph set. The N_{arom} and the anti-hydrogen of the amide moiety of INM molecules interact with one of the O−H moieties (O−H···N_{arom}: 2.688 (3) Å) and the carbonyl moieties (O···N−H: 3.019 (3) Å) of the QUE molecule respectively. The supramolecular interactions between QUE and INM molecules in the QUEINM cocrystal overall lead to the generation of a 2-D sheet as shown in Figure 5.

QUECAF·MeOH. This cocrystal crystallizes in the $P2_1/c$ space group. The N_{arom} of the imidazole ring and the CO of the imide ring of CAF interact with O−H moieties of QUE through O−H···N_{arom} (2.821 (3) Å) and CO···O−H (2.716 (3) Å)

Table 2. Crystallographic Data and Structure Refinement Parameters for the Cocrystals Reported Herein

	QUEINM	QUECAF·MeOH
formula	$C_{21}H_{16}N_2O_8$	$C_{24}H_{24}N_4O_{10}$
MW	424.36	528.47
crystal system	triclinic	monoclinic
space group	$P\bar{1}$	$P2(1)/c$
a (Å)	4.978 (1)	10.309 (3)
b (Å)	12.636 (3)	14.853 (4)
c (Å)	15.571 (3)	15.199 (5)
α (deg)	110.53 (3)	90
β (deg)	97.63 (3)	100.612 (2)
γ (deg)	99.39 (3)	90
V/Å^3	885.7 (3)	2287.51 (12)
D_c/mg m^{-3}	1.5913	1.535
Z	2	4
2θ range	2.66 to 24.93	4.20 to 67.88
Nref/Npara	2999/292	4031/353
T/K	100 (2)	100 (2)
R_1 [$I > 2\sigma(I)$]	0.0592	0.0434
wR_2	0.1267	0.1090
GOF	1.091	1.035
abs coeff	0.124	0.1033

Table 3. Selected Hydrogen Bond Distances and Parameters for the Cocrystals Reported Herein

cocrystal	hydrogen bond	d(H···A)/Å	D(D···A)/Å	θ/deg
QUEINM	O−H···N	1.86	2.688 (3)	167.2
	O−H···O	1.91	2.658 (3)	147.2
	O−H···O	2.25	2.710 (3)	114.2
	O−H···O	2.01	2.765 (3)	149.5
	O−H···O	2.27	2.712 (3)	113.2
	O−H···O	1.78	2.610 (3)	171.6
	N−H···O	2.15 (4)	3.028 (4)	170 (3)
	N−H···O	2.17 (4)	3.019 (4)	178 (4)
QUECAF·MeOH	O−H···N	2.04	2.820 (2)	154.8
	O−H···O	2.26	2.708 (2)	113.6
	O−H···O	2.43	2.843 (2)	111.4
	O−H···O	1.85	2.598 (2)	148.4
	O−H···O	1.88	2.719 (2)	173.1
	O−H···O	1.96	2.773 (2)	163.5
	O−H···O	1.79	2.629 (2)	174.9
	O−H···O	2.31	2.751 (2)	113.4
	O−H···O	1.88	2.712 (2)	169.4

hydrogen bonds. Both the O−H in the catechol moiety of the QUE molecule hydrogen bond to the O−H of a neighboring QUE molecule through O−H···O and O···O−H ((2.774 (3) 353 Å and 2.847 (3) Å supramolecular heterosynthons, respectively. One of the O−H adjacent to the CO functionality of the QUE molecule engages in strong intramolecular H-bonding (2.602 (3) Å). The methanol molecule interacts with the remaining CO group on the imide ring of a CAF molecule with

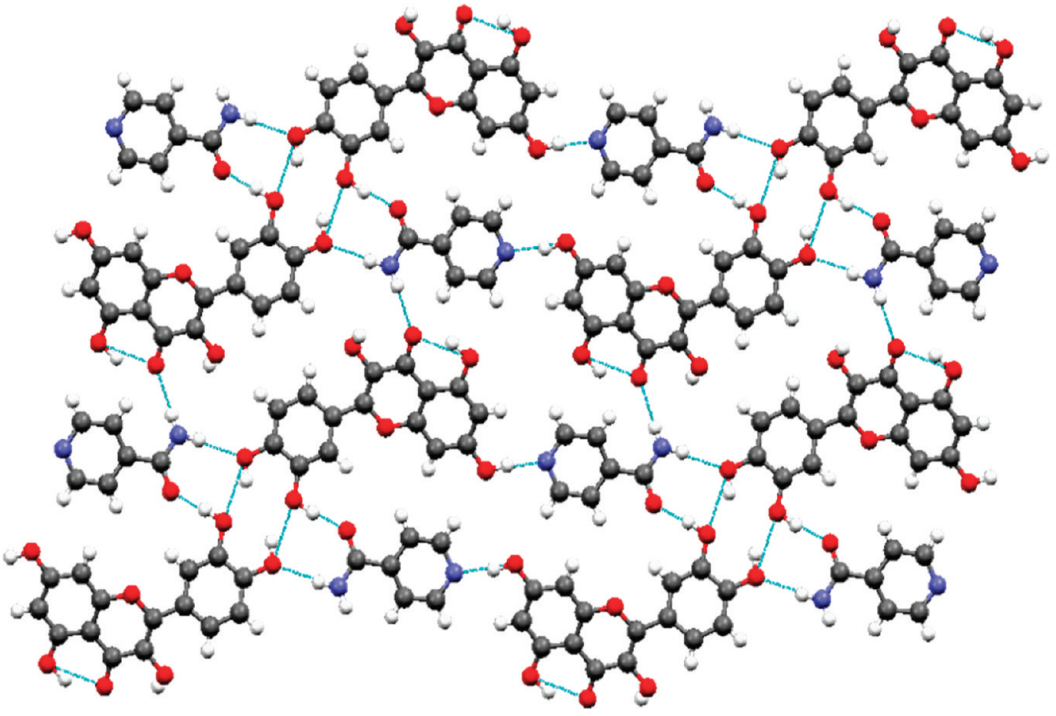

Figure 5. Representation of supramolecular sheet in QUEINM. In the cocrystal the QUE and INM molecules interact via O−H···N_{arom} supramolecular H-bonds. Two QUE molecules form the catechol dimer through O−H···O H-bonds and the amide functionalities of the INM molecules H-bond on either side of the catechol dimer. Overall H-bonding results in the generation of supramolecular sheet.

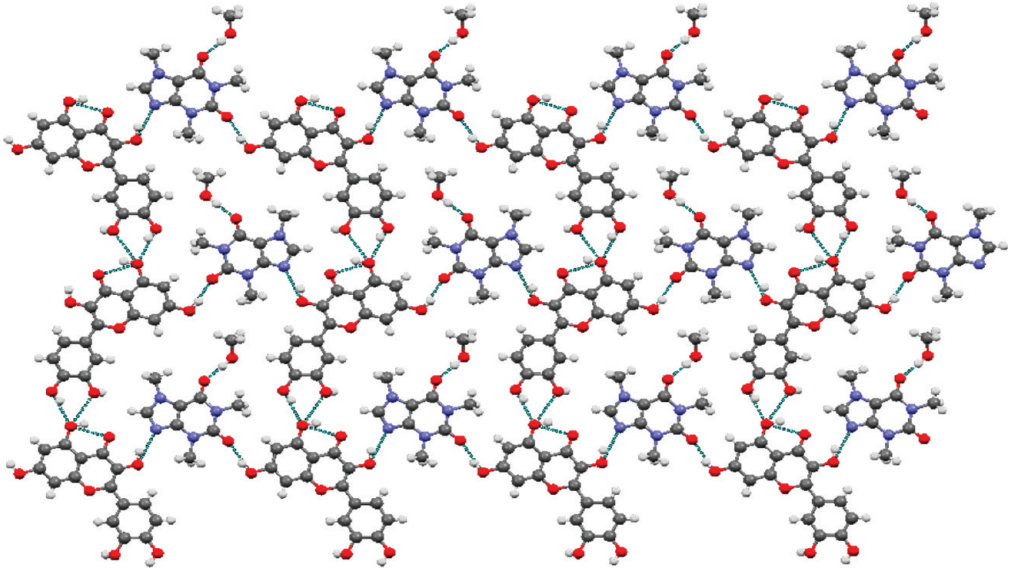

Figure 6. Intermolecular hydrogen bonding in QUECAF·MeOH. QUE molecules interact with CAF molecules through O−H···N_{arom} and O−H···C═O supramolecular H-bonds, and the MeOH molecules just interact with the CAF molecules. A supramolecular sheet is produced by hydrogen bonding between QUE, CAF and MeOH molecules.

a hydrogen bond distance of 2.712 (3) Å. The overall interactions between QUE, CAF and MeOH result in the formation of a supramolecular sheet as shown in Figure 6. The MeOH molecules in one layer interact with one of the O−H of the catechol moieties of QUE in another supramolecular sheet through O···O−H hydrogen bonds. This results in the formation of bilayers as shown in Figure 7.

The crystal structure of QUETBR·$2H_2O$ has been published elsewhere.[45] The crystal structure of QUECAF has not been determined yet, but the chemical identity of the cocrystal is confirmed from the PXRD, IR, DSC and TGA. The PXRD reveals that QUECAF is isostructural to QUECAF·MeOH (Figure 8a), and the DSC confirms that after the loss of MeOH molecule from QUECAF·MeOH the cocrystal is still

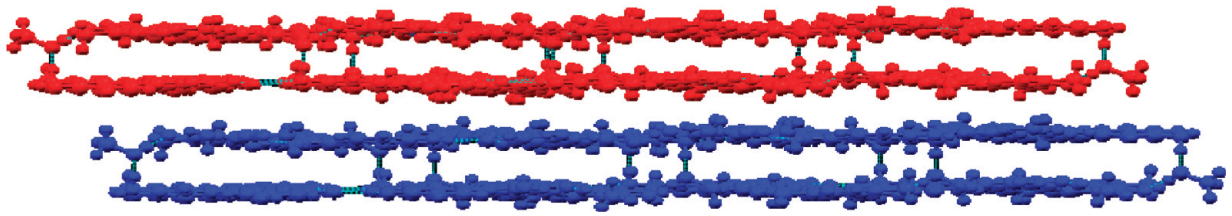

Figure 7. Illustration of bilayers in QUECAF·MeOH. Each supramolecular sheet in QUECAF·MeOH interacts with the other other sheets through MeOH molecules and results in the formation of bilayers which can be described as ABAB and so on.

stable and has the same melting point as that of the solvated one (Figure 8b).

DISCUSSION

Given that QUE exhibits numerous useful bioactivities it is not surprising that it continues to be studied even after the discovery of its poor bioavailability in 1975.[19] Since then, there have been several follow-up reports of QUE deposition and bioavailability in various animal models.[10,11,16−18,46−48] The reoccurring theme in the existing literature is that QUE is present in systemic circulation mainly as conjugated metabolites. Piskula et al. (1998) studied the bioavailability of QUE in various vehicles in a rat model and reported circulating levels of QUE and its metabolites.[49] Not surprisingly, the free, unconjugated QUE was detected only when QUE was administered in a propylene glycol vehicle, in which it was most soluble compared to the other vehicles. They later hypothesized that this phenomenon was likely due to animals' overdosing. It is not clear whether they meant experimental error (animals given more than 50 mg/kg) or a saturation of liver first pass enzymes due to more rapid absorption in the vehicle that exhibited the highest solubility. Either of these is a feasible explanation. Nonetheless, it was clear that QUE was present *in vivo* mainly as a conjugated metabolite and that its solubility was an important factor in overall absorption. The premise that modulating the solubility of QUE could affect its absorption is what fueled our study and others before it. Kim et al (2009) reported several new quercetin−amino acid conjugates that exhibited improved water solubility and *in vitro* stability and permeability.[50] Even though this will presumably lead to improved bioavailability, this remains to be seen due to the lack of an *in vivo* evaluation.

In this study, we evaluated the bioavailability of four cocrystals of QUE with varying degrees of improved water solubility in comparison to QUE alone. Our *in vivo* pharmacokinetic evaluation is in agreement with existing literature in that modulating solubility did impact absorption patterns of the QUE cocrystals. Since solubility often limits the rate of absorption of a compound, one would expect that improving the solubility of a poorly soluble compound would shift to the left the time at which maximal plasma levels were achieved. This was the case for all of the cocrystals presented in this study. In Table 1, the QUE dihydrate control had a T_{MAX} of 30 min, whereas the cocrystals peaked at 5 and 10 min. Not only did the QUE cocrystals reach systemic circulation more quickly than QUE dihydrate but they also reached significantly higher concentrations. The QUECAF·MeOH cocrystal peaked rapidly at 5 min with 7.7 μM free QUE. For comparison, the QUE dihydrate control peaked at 30 min with 0.84 μM QUE aglycon.

Even though solubility is a limiting factor of the oral bioavailability of QUE, it is apparent that it is not the only factor. Modulation of metabolism can also have drastic effects on oral bioavailability. Recently, one study reported that several ester-based precursors to QUE might be useful for increasing systemic aglycon concentrations.[51] The investigators demonstrated that some ester precursors were resistant to phase II conjugation by tight monolayers of MDCK-1, MDCK-2, and Caco-2 cells. They hypothesize that *in vivo* the residual acyl groups will be eliminated leaving the QUE aglycon that is known to be bioactive. Although this data is promising, the study is limited due to the lack of *in vivo* evaluation. Additionally, one of the major limitations to QUE is its very low water solubility. Each of these precursors was reported to exhibit solubility similar to QUE. This might pose a formulation dilemma due to insolubility and poor dissolution at physiologically relevant doses *in vivo*.

Interestingly, post hoc analysis of the pharmacokinetic curve (Figure 4) revealed that modulation of solubility is probably not the only contributing factor to the improved bioavailability of some of the QUE cocrystals. This is evident when the relative solubilities of each cocrystal (Figure 3) are compared to the pharmacokinetic profile (Figure 4). Based on solubility differences alone, the QUECAF cocrystal would be expected to have the highest C_{MAX} since it would be solubilized, and thus absorbed, more completely than the others. However, the QUECAF cocrystal had the lowest C_{MAX} of all of the cocrystals, peaking at just 656 ng/mL at 10 min. Furthermore, the QUEINM cocrystal had the second lowest solubility and caused systemic QUE aglycon levels to reach 1401 ng/mL, second only to the QUECAF·MeOH cocrystal. Therefore, there must be factors other than solubility at play. It is possible that the INM might reduce the first pass effect of the liver enzymes on QUE. Perhaps most interesting is the pharmacokinetic profile of the QUETBR·2H_2O cocrystal (Figure 4). Despite having a solubility that is only slightly higher than that of QUE dihydrate, this cocrystal achieved sustained levels of quercetin aglycon, indicative of modulated elimination. The resultant F_{REL} of the QUETBR·2H_2O cocrystal was 9.93, the largest increase observed in this study (Table 1). This cocrystal also exhibited the longest E $T_{1/2}$, 145 min (Table 1). Still, we cannot reach any definitive conclusion about the metabolism of the cocrystals since we did not measure circulating QUE metabolites.

These results add to existing evidence that cocrystallization is a useful methodology for improving the physicochemical properties of a compound and that these improvements can lead to drastically enhanced bioavailability when applied to compounds that are limited by their solubility. This same ideology was previously shown to be successful in several preclinical studies. Carbamazepine (CBZ) is used for the treatment of epilepsy and bipolar disorder but also suffers from low solubility and oral bioavailability. Cocrystals of CBZ and saccharin were administered orally to dogs and were found to achieve greater plasma concentrations than the API alone.[30] This improvement in

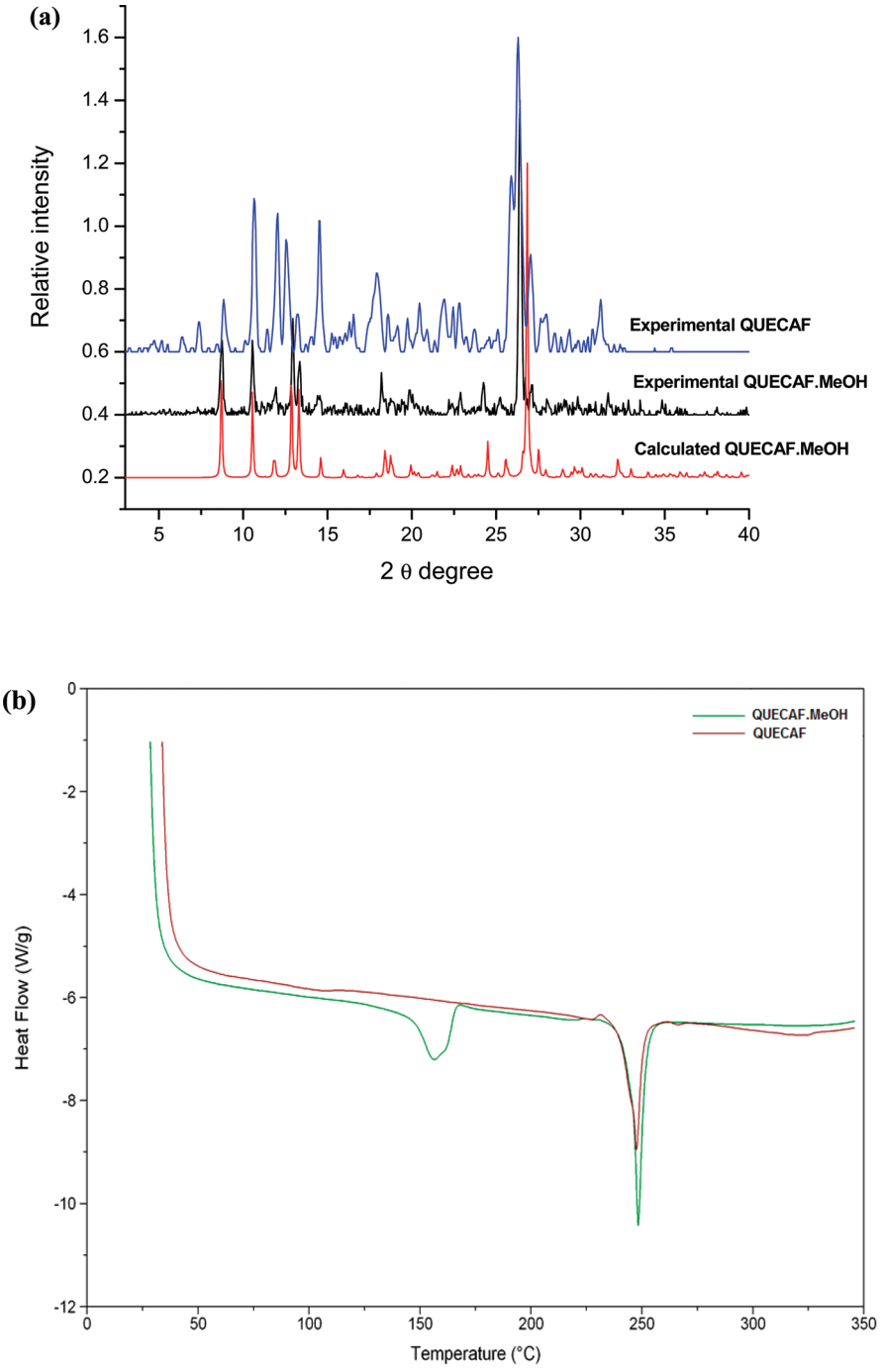

Figure 8. (a) Comparison PXRDs of QUECAF·MeOH and QUECAF. (b) Comparison of DSCs of QUECAF·MeOH and QUECAF. The PXRD patterns of QUECAF·MeOH calculated and experimental (bulk powder) match exactly, indicating the total conversion of the starting materials into cocrystal and no presence of starting materials. The similarity in the PXRD patterns of QUECAF·MeOH and QUECAF indicates isostructural nature of both cocrystals. Similarly, the DSC of QUECAF reveals that the crystal packing is intact even after the removal of MeOH molecule as its melting point matches with that of QUECAF·MeOH.

bioavailability was attributed to the improved solubility of the cocrystal. AMG 517, VR1 (vanilloid receptor 1) antagonist is a practically insoluble drug, which limits its bioavailability. Bak et al. reported that the cocrystallization of AMG 517 with sorbic acid dramatically increases its bioavailability in rats.[31] Similarly, Jung et al. used cocrystallization to improve the solubility, and consequent bioavailability of indomethacin.[52] Thus, modulating the solubility of a poorly soluble API using cocrystallization appears to be a proven, highly effective, and broadly applicable method for improving oral bioavailability.

Taken with the existing evidence from the literature, the results of this study further implicate the potential for cocrystallization in drug development. One limitation is that the plasma samples were analyzed for free, unconjugated QUE content

alone. This is because modulated metabolism was not an expected outcome of cocrystallization. However, given the unexpected discrepancies between the solubility and pharmacokinetic profiles of the cocrystals, modulated metabolism is probable. Future studies should investigate whether cocrystallization with certain cocrystal formers can be used to modulate the metabolism of the API. Nevertheless, this study implicates cocrystallization as a potential solution to the solubility and bioavailability problems that thwart the success of QUE as an effective treatment option for its numerous clinical indications.

■ ASSOCIATED CONTENT

Supporting Information. Crystallographic information files (CIF) for the QUECAF·MeOH and QUEINM cocrystals and IR, DSC, and PXRD data for each cocrystal. This material is available free of charge via the Internet at http://pubs.acs.org.

■ AUTHOR INFORMATION

Corresponding Authors

*M.J.Z.: Department of Chemistry, University of South Florida, College of Arts and Sciences, Tampa, FL, USA 33612; phone, 813-974-3451; e-mail, zaworo@cas.usf.edu. R.D.S.: Center of Excellence in Aging and Brain Repair, MDC78, Department of Neurosurgery and Brain Repair, University of South Florida, College of Medicine, Tampa, FL, USA 33612; phone, 813-974-9171; fax, 813-974-3078; e-mail: dshytle@health.usf.edu.

■ ACKNOWLEDGMENT

This work was supported by research grant number ARG2008 from the Johnnie B. Byrd, Sr. Alzheimer's Center & Research Institute (R.D.S. and M.J.Z.).

■ ABBREVIATIONS USED

QUE, quercetin; QUECAF, quercetin:caffeine; QUECAF·MeOH, quercetin:caffeine:methanol; QUEINMquercetin:isonicotinamide, quercetin:isonicotinamide; QUETBR·2H_2O, quercetin:theobromine dehydrate; API, active pharmaceutical ingredient; INM, isonicotinamide; CAF, caffeine; TBR, theobromine; PXRD, powder X-ray diffraction; DSC, differential scanning calorimeter; FT-IR, infrared spectroscopy; AUC, area under curve; F_{REL}, relative bioavailability; A $T_{1/2}$, absorption half-life; D $T_{1/2}$, distribution half-life; E $T_{1/2}$, elimination half-life

■ REFERENCES

(1) Hertog, M. G. Epidemiological evidence on potential health properties of flavonoids. *Proc. Nutr. Soc.* **1996**, *55*, 385–97.

(2) Arts, I. C. A review of the epidemiological evidence on tea, flavonoids, and lung cancer. *J. Nutr.* **2008**, *138*, 1561S–1566S.

(3) Egert, S.; Wolffram, S.; Bosy-Westphal, A.; Boesch-Saadatmandi, C.; Wagner, A. E.; Frank, J.; Rimbach, G.; Mueller, M. J. Daily quercetin supplementation dose-dependently increases plasma quercetin concentrations in healthy humans. *J. Nutr.* **2008**, *138*, 1615–21.

(4) Formica, J. V.; Regelson, W. Review of the biology of Quercetin and related bioflavonoids. *Food Chem. Toxicol.* **1995**, *33*, 1061–80.

(5) Murakami, A.; Ashida, H.; Terao, J. Multitargeted cancer prevention by quercetin. *Cancer Lett.* **2008**, *269*, 315–25.

(6) Spencer, J. P.; Kuhnle, G. G.; Williams, R. J.; Rice-Evans, C. Intracellular metabolism and bioactivity of quercetin and its in vivo metabolites. *Biochem. J.* **2003**, *372*, 173–81.

(7) Vargas, A. J.; Burd, R. Hormesis and synergy: pathways and mechanisms of quercetin in cancer prevention and management. *Nutr. Rev. 68*, 418-28.

(8) Bakay, M.; Mucsi, I.; Beladi, I.; Gabor, M. Effect of flavonoids and related substances. II. Antiviral effect of quercetin, dihydroquercetin and dihydrofisetin. *Acta Microbiol. Acad. Sci. Hung.* **1968**, *15*, 223–7.

(9) Leopoldini, M.; Russo, N.; Chiodo, S.; Toscano, M. Iron chelation by the powerful antioxidant flavonoid quercetin. *J. Agric. Food Chem.* **2006**, *54*, 6343–51.

(10) Ader, P.; Wessmann, A.; Wolffram, S. Bioavailability and metabolism of the flavonol quercetin in the pig. *Free Radical Biol. Med.* **2000**, *28*, 1056–67.

(11) Cermak, R.; Landgraf, S.; Wolffram, S. The bioavailability of quercetin in pigs depends on the glycoside moiety and on dietary factors. *J. Nutr.* **2003**, *133*, 2802–7.

(12) Erlund, I.; Freese, R.; Marniemi, J.; Hakala, P.; Alfthan, G. Bioavailability of quercetin from berries and the diet. *Nutr. Cancer* **2006**, *54*, 13–7.

(13) Graefe, E. U.; Derendorf, H.; Veit, M. Pharmacokinetics and bioavailability of the flavonol quercetin in humans. *Int. J. Clin. Pharmacol. Ther.* **1999**, *37*, 219–33.

(14) Graefe, E. U.; Wittig, J.; Mueller, S.; Riethling, A. K.; Uehleke, B.; Drewelow, B.; Pforte, H.; Jacobasch, G.; Derendorf, H.; Veit, M. Pharmacokinetics and bioavailability of quercetin glycosides in humans. *J. Clin. Pharmacol.* **2001**, *41*, 492–9.

(15) Hollman, P. C.; van Trijp, J. M.; Buysman, M. N.; van der Gaag, M. S.; Mengelers, M. J.; de Vries, J. H.; Katan, M. B. Relative bioavailability of the antioxidant flavonoid quercetin from various foods in man. *FEBS Lett.* **1997**, *418*, 152–6.

(16) Lesser, S.; Cermak, R.; Wolffram, S. Bioavailability of quercetin in pigs is influenced by the dietary fat content. *J. Nutr.* **2004**, *134*, 1508–11.

(17) Manach, C.; Morand, C.; Demigne, C.; Texier, O.; Regerat, F.; Remesy, C. Bioavailability of rutin and quercetin in rats. *FEBS Lett.* **1997**, *409*, 12–6.

(18) Manach, C.; Texier, O.; Morand, C.; Crespy, V.; Regerat, F.; Demigne, C.; Remesy, C. Comparison of the bioavailability of quercetin and catechin in rats. *Free Radical Biol. Med.* **1999**, *27*, 1259–66.

(19) Gugler, R.; Leschik, M.; Dengler, H. J. Disposition of quercetin in man after single oral and intravenous doses. *Eur. J. Clin. Pharmacol.* **1975**, *9*, 229–34.

(20) Reinboth, M.; Wolffram, S.; Abraham, G.; Ungemach, F. R.; Cermak, R. Oral bioavailability of quercetin from different quercetin glycosides in dogs. *Br. J. Nutr.* **2010**, *104*, 198–203.

(21) Shan, N.; Zaworotko, M. J. The role of cocrystals in pharmaceutical science. *Drug Discovery Today* **2008**, *13*, 440–6.

(22) Sarma, B.; Chen, J.; Hsi, H.-Y.; Myerson, A. S. Solid forms of pharmaceuticals: Polymorphs, salts and cocrystals. *Korean J. Chem. Eng.* **2011**, *28*, 315–322.

(23) Basavoju, S.; Bostrom, D.; Velaga, S. P. Indomethacin-saccharin cocrystal: design, synthesis and preliminary pharmaceutical characterization. *Pharm. Res.* **2008**, *25*, 530–41.

(24) Brader, M. L.; Sukumar, M.; Pekar, A. H.; McClellan, D. S.; Chance, R. E.; Flora, D. B.; Cox, A. L.; Irwin, L.; Myers, S. R. Hybrid insulin cocrystals for controlled release delivery. *Nat. Biotechnol.* **2002**, *20*, 800–4.

(25) Cheney, M. L.; Weyna, D. R.; Shan, N.; Hanna, M.; Wojtas, L.; Zaworotko, M. J. Coformer selection in pharmaceutical cocrystal development: A case study of a meloxicam aspirin cocrystal that exhibits enhanced solubility and pharmacokinetics. *J. Pharm. Sci.* **2010**, DOI: 10.1002/jps.22434.

(26) McNamara, D. P.; Childs, S. L.; Giordano, J.; Iarriccio, A.; Cassidy, J.; Shet, M. S.; Mannion, R.; O'Donnell, E.; Park, A. Use of a glutaric acid cocrystal to improve oral bioavailability of a low solubility API. *Pharm. Res.* **2006**, *23*, 1888–97.

(27) Remenar, J. F.; Morissette, S. L.; Peterson, M. L.; Moulton, B.; MacPhee, J. M.; Guzman, H. R.; Almarsson, O. Crystal engineering of novel cocrystals of a triazole drug with 1,4-dicarboxylic acids. *J. Am. Chem. Soc.* **2003**, *125*, 8456–7.

(28) Yadav, A. V.; Dabke, A. P.; Shete, A. S. Crystal engineering to improve physicochemical properties of mefloquine hydrochloride. *Drug Dev. Ind. Pharm.* **2010**, *36*, 1036–45.
(29) Childs, S. L.; Chyall, L. J.; Dunlap, J. T.; Smolenskaya, V. N.; Stahly, B. C.; Stahly, G. P. Crystal engineering approach to forming cocrystals of amine hydrochlorides with organic acids. Molecular complexes of fluoxetine hydrochloride with benzoic, succinic, and fumaric acids. *J. Am. Chem. Soc.* **2004**, *126*, 13335–42.
(30) Hickey, M. B.; Peterson, M. L.; Scoppettuolo, L. A.; Morrisette, S. L.; Vetter, A.; Guzman, H.; Remenar, J. F.; Zhang, Z.; Tawa, M. D.; Haley, S.; Zaworotko, M. J.; Almarsson, O. Performance comparison of a co-crystal of carbamazepine with marketed product. *Eur. J. Pharm. Biopharm.* **2007**, *67*, 112–9.
(31) Bak, A.; Gore, A.; Yanez, E.; Stanton, M.; Tufekcic, S.; Syed, R.; Akrami, A.; Rose, M.; Surapaneni, S.; Bostick, T.; King, A.; Neervannan, S.; Ostovic, D.; Koparkar, A. The co-crystal approach to improve the exposure of a water-insoluble compound: AMG 517 sorbic acid co-crystal characterization and pharmacokinetics. *J. Pharm. Sci.* **2008**, *97*, 3942–56.
(32) *APEX2*; Bruker AXS, Inc.: Madison, WI, 2010.
(33) *SAINT. Data Reduction Software*; Bruker AXS Inc.: Madison, WI, 2009.
(34) Sheldrick, G. M. *SADABS. Program for Empirical Absorption Correction*; University of Gottingen: Germany, 2008.
(35) Farrugia, L. J. *Appl. Crystallogr.* **1999**, *32*, 837–838.
(36) Sheldrick, G. M. *SHELXL-97. program for the Refinement of Crystal*, 1997.
(37) Sheldrick, G. M. *Acta Crystallogr.* **1990**, *A46*, 467–73.
(38) Srinivas, K.; King, J. W.; Howard, L. R.; Monrad, J. k. Solubility and solution thermodynamic properties of quercetin and quercetin dihydrate in subcritical water. *J. Food Eng.* **2010**, *100*, 208–218.
(39) Lambert, J. D.; Lee, M. J.; Diamond, L.; Ju, J.; Hong, J.; Bose, M.; Newmark, H. L.; Yang, C. S. Dose-dependent levels of epigallocatechin-3-gallate in human colon cancer cells and mouse plasma and tissues. *Drug Metab. Dispos.* **2006**, *34*, 8–11.
(40) Wang, L.; Morris, M. E. Liquid chromatography-tandem mass spectroscopy assay for quercetin and conjugated quercetin metabolites in human plasma and urine. *J. Chromatogr., B: Anal. Technol. Biomed. Life Sci.* **2005**, *821*, 194–201.
(41) Wang, M.; Miksa, I. R. Multi-component plasma quantitation of anti-hyperglycemic pharmaceutical compounds using liquid chromatography-tandem mass spectrometry. *J. Chromatogr., B: Anal. Technol. Biomed. Life Sci.* **2007**, *856*, 318–27.
(42) Wang, Z.; Hop, C. E.; Leung, K. H.; Pang, J. Determination of in vitro permeability of drug candidates through a caco-2 cell monolayer by liquid chromatography/tandem mass spectrometry. *J Mass Spectrom* **2000**, *35*, 71–6.
(43) Sparidans, R. W.; Lagas, J. S.; Schinkel, A. H.; Schellens, J. H.; Beijnen, J. H. Liquid chromatography-tandem mass spectrometric assays for salinomycin in mouse plasma, liver, brain and small intestinal contents and in OptiMEM cell culture medium. *J. Chromatogr., B: Anal. Technol. Biomed. Life Sci.* **2007**, *855*, 200–10.
(44) Etter, M. C.; MacDonald, J. C.; Bernstein, J. Graph-set analysis of hydrogen-bond patterns in organic crystals. *Acta Crystallogr., B* **1990**, *46* (Part 2), 256−62.
(45) Clarke, H. D.; Arora, K. K.; Bass, H.; Kavuru, P.; Ong, T. T.; Pujari, T.; Wojtas, L.; Zaworotko, M. J. Structure−Stability Relationships in Cocrystal Hydrates: Does the Promiscuity of Water Make Crystalline Hydrates the Nemesis of Crystal Engineering? *Cryst Growth Des.* **2010**, *10*, 2152–2167.
(46) Mullen, W.; Rouanet, J. M.; Auger, C.; Teissedre, P. L.; Caldwell, S. T.; Hartley, R. C.; Lean, M. E.; Edwards, C. A.; Crozier, A. Bioavailability of [2-(14)C]quercetin-4′-glucoside in rats. *J. Agric. Food Chem.* **2008**, *56*, 12127–37.
(47) Khaled, K. A.; El-Sayed, Y. M.; Al-Hadiya, B. M. Disposition of the flavonoid quercetin in rats after single intravenous and oral doses. *Drug Dev. Ind. Pharm.* **2003**, *29*, 397–403.
(48) Morand, C.; Manach, C.; Crespy, V.; Remesy, C. Respective bioavailability of quercetin aglycone and its glycosides in a rat model. *Biofactors* **2000**, *12*, 169–74.
(49) Piskula, M.; Terao, J. Quercetin's Solubility Affects Its Accumulation in Rat Plasma after Oral Administration. *J. Agric. Food Chem.* **1998**, *46*, 4313–4317.
(50) Kim, M. K.; Park, K. S.; Yeo, W. S.; Choo, H.; Chong, Y. In vitro solubility, stability and permeability of novel quercetin-amino acid conjugates. *Bioorg. Med. Chem.* **2009**, *17*, 1164–71.
(51) Biasutto, L.; Marotta, E.; De Marchi, U.; Zoratti, M.; Paradisi, C. Ester-based precursors to increase the bioavailability of quercetin. *J. Med. Chem.* **2007**, *50*, 241–53.
(52) Jung, M. S.; Kim, J. S.; Kim, M. S.; Alhalaweh, A.; Cho, W.; Hwang, S. J.; Velaga, S. P. Bioavailability of indomethacin-saccharin cocrystals. *J. Pharm. Pharmacol.* **2010**, *62*, 1560–8.